Effects of salt and nickel ion on the conformational stability of *Bacillus pasteurii* UreE

Yeon-Hee Lee[a], Hyung-Sik Won[a], Mann-Hyung Lee[b], Bong-Jin Lee[a,*]

[a] *Research Institute of Pharmaceutical Science, College of Pharmacy, Seoul National University, San 56-1, Shinlim-Dong, Kwanak-Gu, Seoul 151-742, South Korea*

[b] *College of Pharmacy, Catholic University of Daegu, Kyongsan, Kyugbook 712-702, South Korea*

Received 11 April 2002; revised 28 May 2002; accepted 28 May 2002

First published online 10 June 2002

Edited by Hans Eklund

Abstract UreE, a urease accessory protein, is proposed to be a metallochaperone assisting the nickel incorporation into the urease active site. We investigated the effects of salt and nickel on the conformational stability of the UreE from *Bacillus pasteurii* (*Bp*UreE), by circular dichroism (CD) and nuclear magnetic resonance spectroscopy accompanying a thermodynamic inspection. Far-UV CD spectra of *Bp*UreE showed that both salt and nickel stabilized the ordered structure of the protein. The thermal denaturing of *Bp*UreE showed a bimodal feature with an aggregation process before thermal unfolding. This thermally induced aggregation could be suppressed by the addition of salt up to 50 mM, and the further addition of salt increased the thermal resistance of the protein. The nickel addition also elevated the thermal resistance of *Bp*UreE, although it could not prevent the aggregating process. Additionally, the stoichiometry of a specific nickel binding to *Bp*UreE was revealed as one nickel per dimer. Altogether, the present results establish a rather detailed characterization of the thermostability and nickel-binding property of *Bp*UreE.

Key words: Urease; Metallochaperone; Nickel binding; Circular dichroism; Thermal stability; *Bacillus pasteurii* UreE

1. Introduction

Urease is a nickel-containing heteropolymeric enzyme that catalyzes the hydrolysis of urea to produce ammonia and carbamate [1–3]. Increased pH arising from this reaction is critical to the virulence of several human and animal pathogens [1]. Thus the knowledge of molecular details for this biological system is expected to provide targets for potential drugs able to diminish the negative effects of bacterial urease activity in human health [4]. During the past few years, intense research into the molecular action mechanism of urease has been conducted primarily on the enzymes from *Klebsiella aerogenes* (*Ka*), *Bacillus pasteurii* (*Bp*), and *Helicobacter pylori* (*Hp*). It has been revealed that the proper assembly of this metallocenter is a key step for its maturation, and requires at least four accessory proteins named UreD, UreE, UreF, and UreG [3,5]. These accessory proteins form a series of complexes with urease apo-protein and act as a molecular chaperone for activation, by transporting and inserting nickel ions into the urease active site [6,7]. However, the specific roles of these four accessory proteins are not fully understood.

UreE is proposed to be the only nickel-binding protein among the urease accessory proteins, and thus a metallochaperone that delivers nickel ions to urease [2,8,9]. Many UreE proteins from different species commonly possess a His-rich C-terminal tail that can coordinate nickel ions, but its functional role is still not clear [10–12]. For example, the *Ka*UreE dimer can bind approximately six nickel ions, and its C-terminally truncated form, H144*UreE dimer, which lacks the last 15 residues (10 of which are His), is able to bind two nickel ions only [12–14]. Nevertheless, the truncated H144*UreE displays properties and activity comparable to those of the wild-type *Ka*UreE [13]. Not all UreE proteins feature such a long His-rich C-terminal tail. For example, the C-terminal tail of *Bp*UreE contains only two conserved histidines, and their functional role is still unknown.

Crystal structures of UreE from two different species were solved very recently: dimeric structures of H144*UreE mutants bound no or three copper ions [7], and tetrameric structures of *Bp*UreE bound one zinc ion [9]. Unfortunately, the C-terminal tails were truncated or not visible in these structures. In particular, the crystal structure of *Bp*UreE showed two forms of tetrameric states sharing a zinc ion in the dimer–dimer interface. It has been revealed that the tetrameric state of *Bp*UreE could be formed only with a highly concentrated sample in the presence of metal ions, and the physiologically relevant unit of *Bp*UreE is a dimer, as with *Ka*UreE [9,11]. In the crystal structures, the UreE dimer is built by a head-to-head interaction of two identical monomers. Each monomer is made up of two distinct domains and has a unique tertiary structure, in agreement with the lack of significant sequence similarity with other known proteins.

Since the structure of both the metal-free and the nickel-bound UreE is not available, it remains at present obscure whether and how the nickel binding to UreE affects the structure or stability of the protein. In this work, we investigated the effects of salt and nickel binding on the conformational stability of *Bp*UreE. In addition, the nickel-binding stoichiometry of *Bp*UreE at physiological concentrations was evaluated. This paper reports a spectroscopic characterization of the conformational thermostability of the metal-free and the nickel-bound *Bp*UreE.

*Corresponding author. Fax: (82)-2-872 3632.
E-mail address: lbj@nmr.snu.ac.kr (B.-J. Lee).

0014-5793/02/$22.00
PII: S0014-5793(02)02919-8

2. Materials and methods

2.1. Materials and preparation of BpUreE

Chromatography materials and chemicals were purchased from Amersham Pharmacia Biotech. All other materials including 99.9% D_2O were from Sigma, and either of analytical or biotechnological grade. The plasmid pKBurE was prepared by inserting the coding region of UreE, which was amplified from the plasmid pBU11 using PCR, into the plasmid pBR322 [10]. *Bp*UreE was prepared from the overproducing *Escherichia coli* strain DH5α containing the plasmid pKBurE, by growing the bacteria in M9 minimal medium. For the preparation of [u-^{15}N]*Bp*UreE, the [u-^{15}N]ammonium sulfate was included in the medium as the sole nitrogen source. The purification of *Bp*UreE was performed by sequential application of a phenyl Sepharose column and DEAE Sepharose column chromatography, at pH 7.0. Concentrating of the purified *Bp*UreE solution followed by buffer exchange was performed using centriprep (Amicon). The purity was confirmed by SDS–PAGE, and the concentration of *Bp*UreE dimer was determined spectrophotometrically in the presence of 6 M guanidine–HCl, with $\varepsilon_{280} = 40\,680$ M^{-1} cm^{-1}, which was calculated from the protein sequence and by using the ProtParam program on the web server http://www.expasy.org/tools/protparam.html.

2.2. Far-UV circular dichroism (CD) measurements

All of the CD experiments were performed on a Jasco J-715 spectropolarimeter equipped with a temperature-controlling unit, using a 0.2 cm path-length cell, with a 1 nm bandwidth and 4 s response time. The standard far-UV CD spectra were collected at 20°C with a scan speed of 50 nm/min and 0.5 nm step resolution. Three individual scans taken from 245 to 200 nm were added and averaged, followed by subtraction of the solvent CD signal. The thermally induced conformational change was monitored by measuring the far-UV CD spectra at various temperatures during increase of the temperature from 20 to 90°C at a 60°C/h rate.

2.3. CD temperature scan experiments

Thermal denaturation was monitored by measuring the CD signals at 222 nm (CD_{222}) with increasing temperature from 20 to 90°C. Basically, the temperature scan rate was taken at 60°C/h, but the kinetic response of the *Bp*UreE denaturation process was tested by altering the scan rate from 40 to 80°C/h. The CD signal was recorded at every 0.1°C, and the denaturing temperature (T_d) values were calculated after noise reduction of the data points had been performed using the Standard Analysis program (Jasco package software). T_d was represented as either the critical denaturing temperature ($T_{d,c}$) under low-concentration salt conditions, or the half-denaturing temperature ($T_{d,h}$) under high-concentration salt conditions. $T_{d,c}$ was determined at the temperature with the negative maximum of the CD intensity. $T_{d,h}$ was determined at the temperature with the half-denatured fraction, i.e. where $F_d(T) = 0.5$. The denatured fraction (F_d) at any temperature (T) was defined as

$$F_d(T) = \frac{\{CD(T) - CD_n(T)\}}{\{CD_d(T) - CD_n(T)\}}$$

where CD_n and CD_d, the baseline values for native and denatured protein, were obtained from the extrapolations of the linear least-square fits of the data points from 35 to 50°C and from 75 to 90°C, respectively.

2.4. Nuclear magnetic resonance (NMR) spectroscopy

The conventional 2D-[^{1}H-^{15}N]HSQC (heteronuclear single quantum coherence) spectra of 0.7 mM [u-^{15}N]*Bp*UreE dimer dissolved in 20 mM sodium phosphate buffer (pH 6.5) containing 7% D_2O were obtained at 308 K on a Bruker DRX 600 spectrometer. All of the spectra were processed and visualized using the NMRPipe/NMRDraw software [15] and the NMRView program [16].

3. Results and discussion

3.1. Protein identification

Since alkalophilic *B. pasteurii* has been known for its remarkable urease production [17], its *ure* gene cluster was previously cloned, and subsequently the composition of the accessory genes as well as the precise genetic organization were reported by You et al. [10,18]. Very recently, another independent work on the cloning, sequencing, and analyzing of the *B. pasteurii* urease operon containing all four accessory genes was reported by Ciurli et al. [11]. The molecular characterization results by Ciurli et al. showed that their recombinant *Bp*UreE has a chain length of 147 amino acids, and behaves as a dimer. Since our recombinant *Bp*UreE was based on the previous cloning by You et al. [10] and a different expression system from that by Ciurli et al. [11], we confirmed the amino acid sequence and oligomeric state of our recombinant *Bp*UreE by N-terminal sequencing, mass spectrometry, and ultra-centrifugation. All of the results (data not shown) were well consistent with those by Ciurli et al., except that our isolated *Bp*UreE (expressed in M9 medium) contained no zinc ion observed with the isolated *Bp*UreE (expressed in LB medium) by Ciurli et al.

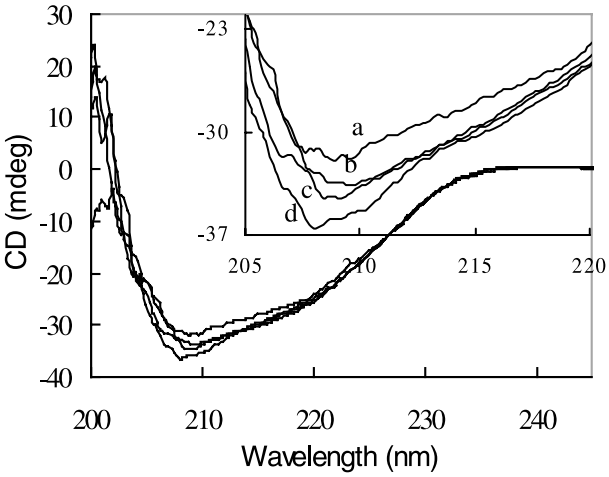

Fig. 1. Effects of salt and Ni^{2+} on the *Bp*UreE conformation. Far-UV CD spectra were obtained at 20°C with 5 μM *Bp*UreE in 20 mM sodium phosphate buffer (pH 6.5) containing no additive (a), and containing 0.5 M NaCl (b), 10 mM $NiCl_2$ (c), and both 0.5 M NaCl and 10 mM $NiCl_2$ (d), respectively. The region from 205 to 220 nm is enlarged in the inset for clarity.

3.2. CD spectroscopy

As shown in Fig. 1, the far-UV CD spectra of *Bp*UreE showed a well-ordered secondary structure of the protein. The CD signals were intensified slightly but reproducibly by the addition of either salt or Ni^{2+}. This indicates that salt and Ni^{2+} contribute to either a conformational change such as coil-to-helix transition, or a stabilization of secondary structure elements, since the signal intensification in this region reflects the more highly ordered secondary structure of a protein [19]. In addition, the co-existence of salt and Ni^{2+} in the protein solution showed a synergic effect on the CD intensification, which suggests that salt and Ni^{2+} probably act with different mechanisms and with no competition.

3.3. Salt effect on the aggregating propensity

The thermal denaturing of *Bp*UreE was monitored by measuring the temperature-dependent CD change at 222 nm, at which CD signals generally reflect the helix content of a protein [20,21]. As shown in Fig. 2A, the thermal denaturation profile of *Bp*UreE in the absence of additive salt showed a bimodal shape with a $T_{d,c}$ at about 59.5°C, which is a unique

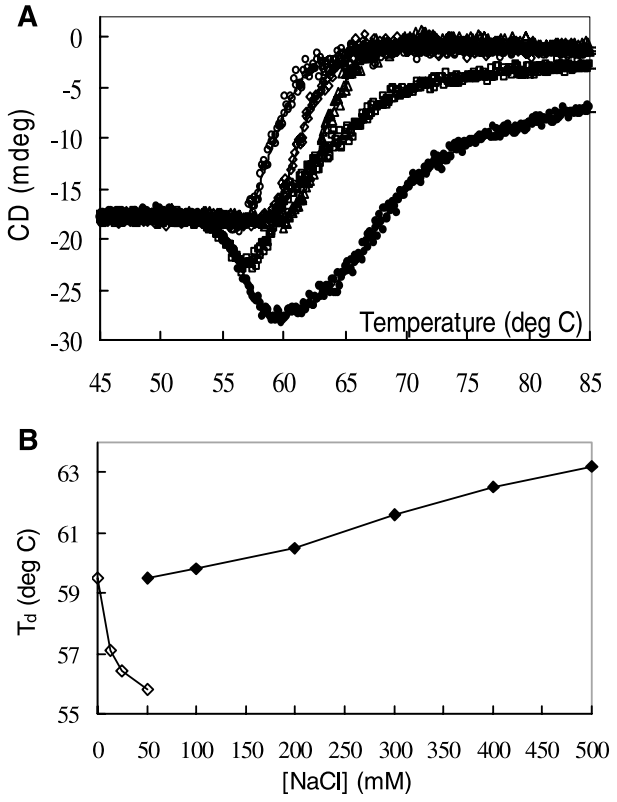

Fig. 2. Effect of salt on the thermal denaturation of *Bp*UreE. CD_{222} values of 4 μM *Bp*UreE in 20 mM sodium phosphate buffer (pH 6.5) were measured over a linear temperature gradient from 10 to 90°C at 60°C/h. Denaturing profile of *Bp*UreE was changed by the addition of salt (A: filled circle, 0 mM; empty rectangle, 12.5 mM; empty circle, 50 mM; empty diamond, 0.3 M; empty triangle, 0.5 M NaCl). The noise-reduced trace of each data set is presented as a solid line curve. The denaturing temperature T_d of each profile was plotted as a function of salt concentration (B: empty symbol, $T_{d,c}$; filled symbol, $T_{d,h}$).

pattern not shown for other known proteins. In particular, the first phase (lower temperature period than the $T_{d,c}$) with intensifying CD signals could be confirmed as neither a stabilizing nor an unfolding process, while the post-$T_{d,c}$ phase with negatively decreasing CD signals seems to depict the unfolding process as generally observed for proteins. In order to identify the first process, we measured far-UV CD spectra of *Bp*UreE at different temperatures during the thermal denaturation period (Fig. 3A). The results revealed that the CD_{222} intensification in the first phase is entirely attributed to the change of the far-UV CD spectral shape, probably due to either a dramatic conformational change such as helix-to-sheet transition or a severe aggregation of the protein. The former possibility is doubtful since the spectral change is too enormous to be expected from a general fashion of a protein conformational change. In contrast, the result of NMR spectroscopy on *Bp*UreE clearly supported the latter assumption.

The [^{1}H-^{15}N]HSQC spectra of the *Bp*UreE (Fig. 4) at high concentration (0.7 mM as dimer) were well dispersed, indicating a well-ordered structure of the protein, as inferred by the far-UV CD spectra (Fig. 1). The agreement between the numbers of peaks and residues in the monomer indicated that the two subunits of *Bp*UreE dimer in solution are symmetric, consistent with the crystal structure [9]. The chemical shifts of individual resonances in the absence of additive salt showed no significant differences from those in the presence of 0.5 M NaCl, which means an invariant *Bp*UreE structure independent of the salt. However, in the absence of additive salt, the protein precipitated gradually during NMR measurement at 308 K for several hours, resulting in a severe reduction of spectral quality (i.e. decrease of sensitivity and resolution), while a good spectrum was obtained with no precipitation in the presence of 0.5 M NaCl salt. The aggregation process of *Bp*UreE in the absence of salt seems to be kinetically driven since the precipitation during NMR measurement was time-dependent.

The kinetic control of the *Bp*UreE aggregation in the absence of salt is also supported by the fact that its denaturing profile is varied depending on the temperature scan rate. As depicted in Fig. 5, altering the temperature scan rate from 40 to 80°C/h changed the thermal denaturing curve remarkably in the absence of salt. Accelerating the temperature scan rate, the first phase before $T_{d,c}$ was increased, i.e. $T_{d,c}$ was shifted to a higher temperature and CD_{222} at $T_{d,c}$ was intensified. In addition, the denatured baselines did not match each other, whereas the native baselines are consistent. In contrast, in the presence of 0.5 M NaCl, the denaturing curve showed only a slight shift up to higher temperatures upon increasing scan rate, with no significant change of denatured baseline. This indicates that the high concentration salt effectively suppresses the *Bp*UreE aggregation, thus bringing the thermal denaturation of the protein under a nearly complete thermodynamic control.

Altogether, it was evidenced from the CD and NMR results that the *Bp*UreE has an aggregating propensity at high con-

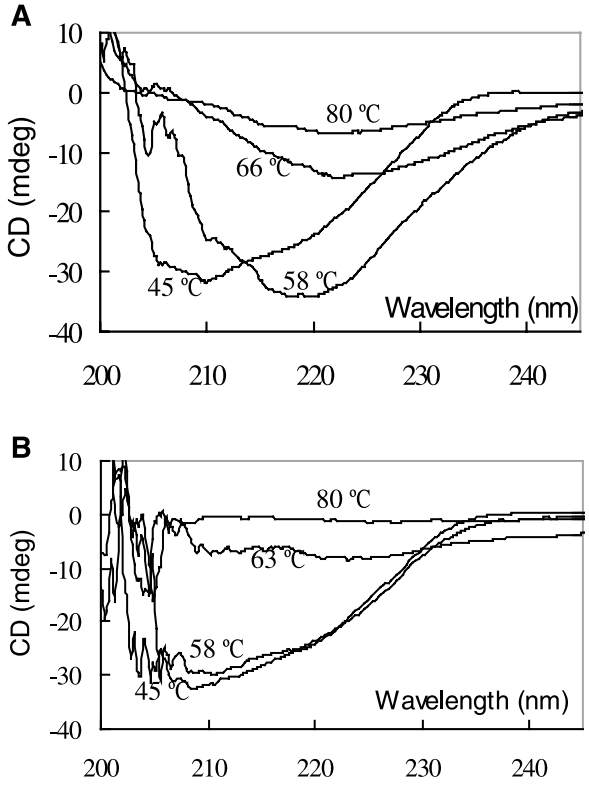

Fig. 3. Conformational change of *Bp*UreE upon increasing temperature. Far-UV CD spectra were measured at different temperatures with 5 μM *Bp*UreE in 20 mM sodium phosphate buffer (pH 6.5) containing no additional salt (A) and 0.5 M NaCl (B), respectively.

centration and/or at high temperature, prior to its unfolding. This aggregating process could be suppressed effectively by the addition of the high concentration salt.

3.4. Stabilizing effect of salt

The effects of salt on the thermal stability of *Bp*UreE structure were further investigated thermodynamically by monitoring the temperature dependence of CD_{222} values. The change in the thermal denaturing profile of *Bp*UreE showed a bimodal dependence on the salt concentration (Fig. 2). Upon increasing concentrations of salt up to about 50 mM, $T_{d,c}$ of *Bp*UreE shifted to lower temperature and the absolute CD intensity at $T_{d,c}$ decreased. Additionally, the denatured baselines of the profiles did not match each other and were upshifted at higher concentrations of salt. However, in the presence of more than 50 mM salt, the first phase before $T_{d,c}$ was negligible, thus making the denaturing curve shape similar with that observed generally for proteins. In addition, the denatured baselines matched each other well, which means that these thermal denaturations came under nearly entire thermodynamic control. In the denaturing temperature period, the far-UV CD spectra in the presence of 0.5 M NaCl (Fig. 3B) did not show the dramatic conversion of shape observed in the absence of salt (Fig. 3A), indicating that the high concentration salt contributed to the suppression of the *Bp*UreE aggregation. The half-denaturing temperature $T_{d,h}$ could be determined apparently in the presence of more than 50 mM salt, and is plotted in Fig. 2B as a function of salt concentration. The increasing $T_{d,h}$ upon increasing concentrations of salt clearly shows that the high concentration salt increased the thermal resistance of *Bp*UreE.

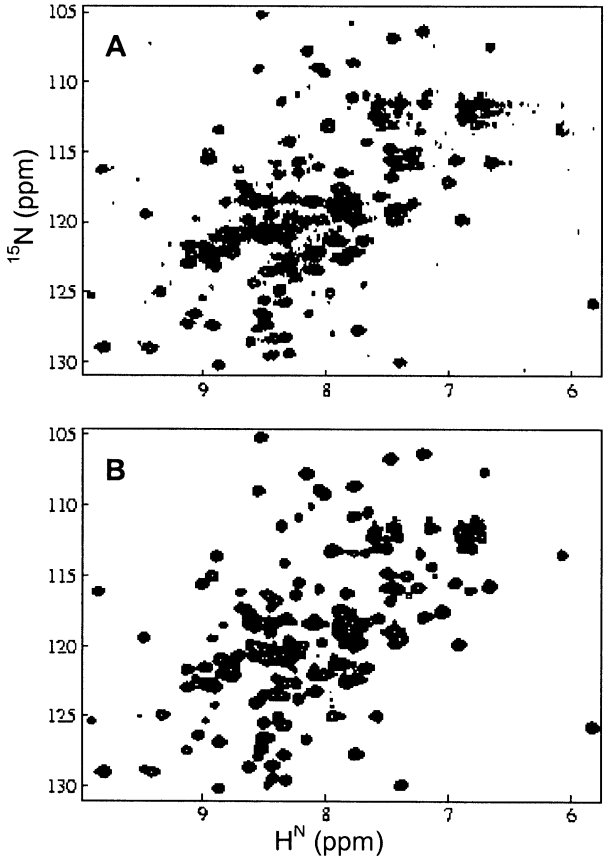

Fig. 4. NMR monitoring of salt effect on the *Bp*UreE conformation. 2D-[^{1}H-^{15}N]HSQC spectra of 0.7 mM *Bp*UreE dimer in 20 mM sodium phosphate buffer (pH 6.5) containing no (A) and 0.5 M (B) NaCl, respectively, were obtained at 308 K.

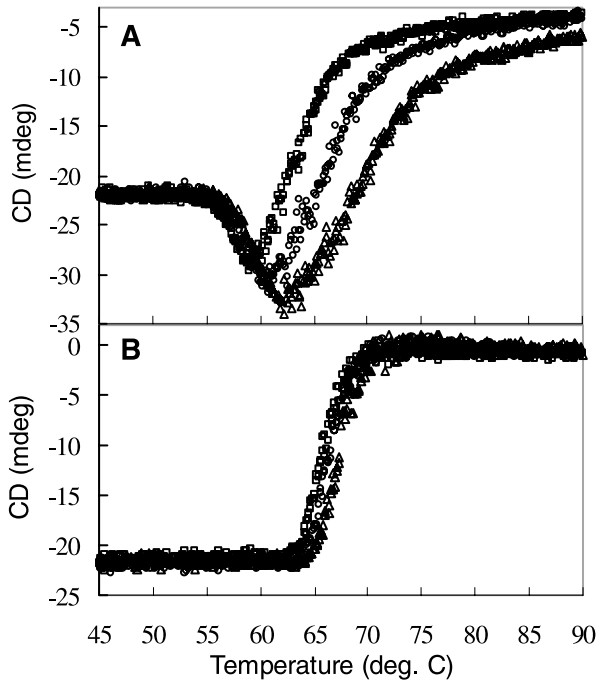

Fig. 5. Effect of the temperature scan rate on the thermal denaturation profile of *Bp*UreE. CD_{222} values of 5 μM *Bp*UreE in 20 mM sodium phosphate buffer (pH 6.5) containing no (A) and 0.5 M NaCl (B) were monitored upon increasing temperature at 40 (rectangle), 60 (circle), and 80°C/h (triangle symbols) rates, respectively.

3.5. Stabilizing effect and stoichiometry of Ni^{2+} binding

The thermal denaturation of the Ni^{2+}-bound *Bp*UreE was also monitored by CD spectroscopy both in the presence and in the absence of salt, respectively. Fig. 6 clearly depicts that the Ni^{2+} binding increased the thermal resistance of *Bp*UreE independently of salt, by shifting the denaturing curve to the higher temperature. In contrast to the salt, Ni^{2+} binding to *Bp*UreE did not change the denaturing pattern, i.e. the preunfolding aggregation process and the mismatching of the denatured baseline were not overcome by Ni^{2+} binding in the absence of salt (Fig. 6A). Thus, the stabilizing effects by Ni^{2+} and salt seem to have a different mechanism, in line with the far-UV CD results shown in Fig. 1.

It has been known that Ni^{2+} binds to UreE with very high affinity of nanomolar K_d [2,15]. Thus, the stoichiometry of Ni^{2+} binding to *Bp*UreE could be deduced from the change of T_d ($T_{d,c}$ in the absence of salt and $T_{d,h}$ in the presence of salt) of the protein as a function of molar ratio of [Ni^{2+}] to [*Bp*UreE]. As shown in Fig. 6C, the dramatic increase of T_d by Ni^{2+} binding was nearly completed at the stoichiometry of approximately one Ni^{2+} ion per *Bp*UreE dimer. The additional Ni^{2+} might bind to *Bp*UreE with no effect on the thermal stability of the protein. The present results, however, indicate that the number of Ni^{2+} that bound specifically to the dimeric *Bp*UreE would not exceed one. This stoichiometry (one Ni^{2+} per dimer) is not consistent with that determined by the crystal structure and the NMR hyperfine shift experiment at high concentrations of *Bp*UreE (2 mM monomer), where the stoi-

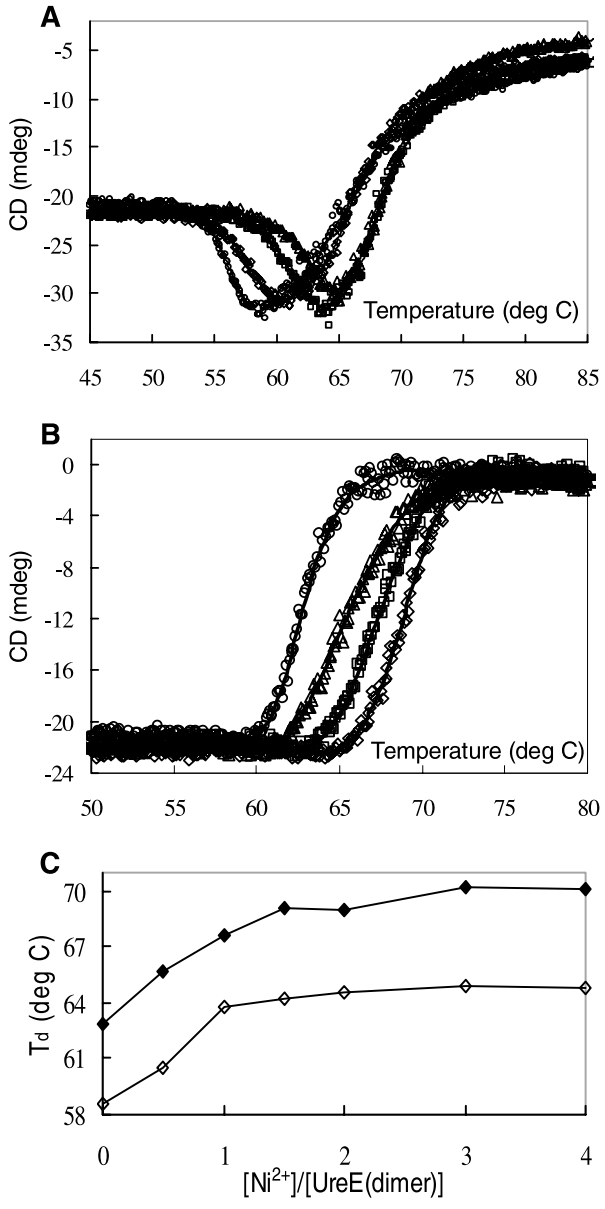

Fig. 6. Effect of Ni^{2+} on the thermal denaturation of *Bp*UreE. CD_{222} values of 5 μM *Bp*UreE in 20 mM sodium phosphate buffer (pH 6.5) were monitored over a linear temperature gradient from 10 to 90°C at 60°C/h. The effect of Ni^{2+} was tested in the absence of additional salt (A) and in the presence of 0.5 M NaCl (B), respectively: empty circle, in the presence of 0 mM; empty triangle, 2.5 mM; empty rectangle, 5 mM; empty diamond, 10 mM $NiCl_2$. The noise-reduced trace of each data set is presented as a solid line curve. The denaturing temperature T_d of each profile was plotted as a function of bound Ni^{2+} (C: empty diamond, $T_{d,c}$ of each profile in the absence of salt; filled diamond, $T_{d,h}$ of each profile in the presence of 0.5 M NaCl).

chiometry of one nickel ion per tetrameric *Bp*UreE was evidenced [9,11]. However, it has been proven that the tetrameric *Bp*UreE is formed only at a high concentration in the presence of metal ion, while the physiological *Bp*UreE behaves as a dimer with no relation to the presence of metal ion [9,11]. The detailed inspection of the present result shows that the stoichiometry of Ni^{2+} binding in the presence of 0.5 M salt is observed over slightly one Ni^{2+} per *Bp*UreE dimer (Fig. 6C). This could be a general aspect due to the reduction of Ni^{2+}-binding affinity by the interference of excess salt.

Since the *Bp*UreE dimer conformation is symmetric in solution, the physiological stoichiometry of one Ni^{2+} per *Bp*UreE dimer indicates that the binding site of Ni^{2+} is probably located at the dimeric interface of the protein. This is also supported by the tetrameric crystal structure of *Bp*UreE, where a zinc ion is bound at the monomer–monomer interface of the physiologically significant dimeric unit, and it also constitutes the dimer–dimer interface of the tetrameric structure. The bound zinc ion in this crystal could be substituted by a nickel ion [9].

3.6. Concluding remarks

The present results clearly showed that the salt and nickel binding to *Bp*UreE contribute to the conformational and thermal stability of the protein. Salt and nickel commonly stabilized the ordered structure of *Bp*UreE and improved the thermal stability of the protein. In addition, salt could suppress the thermally induced aggregation of *Bp*UreE, and the stoichiometry of a specific nickel binding to *Bp*UreE was revealed as one ion per dimer.

Generally the effects of salt on protein structures are observed with various mechanisms, and often not fully understood because of the complexity. In addition, the conformational stabilization by salt is not a common phenomenon of proteins [22,23]. It is likely that the salt effect on *Bp*UreE would be related to the peculiar structure of the protein. The crystal structure of the zinc-bound *Bp*UreE showed a rather amphipathic feature. The one side with the metal-binding center comprises a highly hydrophobic face with some smaller positively charged patches, whereas the opposite side features an extended negatively charged and hydrophilic surface. Particularly, as proposed by Remaut et al. [9], the hydrophobic metal-binding face would be the region most likely involved in the interaction with the preformed super-complex involving the other urease chaperones and apo-urease itself. This would also infer a potential propensity of a self-association of *Bp*UreE, and thus the salt is expected to be able to prevent the aggregation of *Bp*UreE due to the unfavorable self-association. Salt can decrease unfavorable electrostatic interactions between the surface charges, and stabilize the intrahelical salt bridges, thus stabilizing the native state of *Bp*UreE [24,25].

Metal or ligand binding often increases the stability of proteins [19,26–29], but the dramatic stabilization of the *Bp*UreE structure by nickel binding is somewhat unexpected since the nickel is bound probably on the surface of the protein dimer with a limited coordination by His-100 residues only [9]. The stabilizing effects of salt and nickel on the *Bp*UreE structure would be achieved by altering the dynamic property of the protein [29]. The detailed molecular mechanism and the functional role of the *Bp*UreE stabilization by salt and nickel would be worth investigating at the structural level.

Acknowledgements: The authors wish to acknowledge the financial support of the Korea Science and Engineering Foundation (2000-2-20900-010-3, R01-2000-00144). This work was supported in part by the 2002 BK21 project for Medicine, Dentistry, and Pharmacy. We also thank Stefano Ciurli (University of Bologna, Italy) for sharing information about the molecular characterization of *B. pasteurii* UreE prior to publication.

References

[1] Mobley, H.L.T. and Hausinger, R.P. (1989) Microbiol. Rev. 53, 85–108.
[2] Lee, M.-H., Pankratz, H.S., Wang, S., Scott, R.A., Finnegan, M.G., Johnson, M.K., Ippolito, J.A., Christianson, D.W. and Hausinger, R.P. (1993) Protein Sci. 2, 1042–1052.
[3] Park, I.-S. and Hausinger, R.P. (1995) J. Bacteriol. 177, 1947–1951.
[4] Ha, N.-C., Oh, S.-T., Sung, J.-Y., Cha, K.-A., Lee, M.-H. and Oh, B.-H. (2001) Nat. Struct. Biol. 8, 505–509.
[5] Soriano, A., Colpas, G.J. and Hausinger, R.P. (2000) Biochemistry 39, 12435–12440.
[6] O'Halloran, T.V. and Culotta, V.C. (2000) J. Biol. Chem. 275, 25057–25060.
[7] Song, H.K., Bulrooney, S.B., Huber, R. and Hausinger, R.P. (2001) J. Biol. Chem. 276, 49359–49364.
[8] Colpas, G.J. and Hausinger, R.P. (2000) J. Biol. Chem. 275, 10731–10737.
[9] Remaut, H., Safarov, N., Ciurli, S. and Beeumen, J.V. (2001) J. Biol. Chem. 276, 49365–49370.
[10] You, J.-H., Song, B.-H., Kim, J.-G., Lee, M.-H. and Kim, S.-D. (1995) Mol. Cell 5, 359–369.
[11] Ciurli, S., Safarov, N., Miletti, S. and Dikiy, A. (2002) J. Biol. Inorg. Chem. (in press), online first publication (DOI 10.1007/s00775-002-0341-7), URL: http://dx.doi.org/10.1007/s00775-002-0341-7.
[12] Colpas, G.J., Brayman, T.G., Ming, L.-J. and Hausinger, R.P. (1999) Biochemistry 38, 4078–4088.
[13] Brayman, T.G. and Hausinger, R.P. (1996) J. Bacteriol. 178, 5410–5416.
[14] Colpas, G.J., Brayman, T.G., Mccracken, J., Pressler, M.A., Babcock, G.T., Ming, L.-J., Colangelo, C.M., Scott, R.A. and Hausinger, R.P. (1998) J. Biol. Inorg. Chem. 3, 150–160.
[15] Delaglio, F., Grzesiek, S., Vuister, G.W., Zhu, G., Pfeifer, J. and Bax, A. (1995) J. Biomol. NMR 6, 277–293.
[16] Johnson, B.A. and Blevins, R.A. (1994) J. Biomol. NMR 4, 603–614.
[17] Larson, A.D. and Kallio, R.E. (1954) J. Bacteriol. 68, 67–73.
[18] Shin, I.-S. and Lee, M.-H. (1999) J. Microbiol. Biotechnol. 9, 255–259.
[19] Greenfield, N., Vijayanathan, V., Thomas, T.J., Gallo, M.A. and Thomas, T. (2001) Biochemistry 40, 6646–6652.
[20] Park, S.-H., Kim, Y.-K., Park, J.-W., Lee, B. and Lee, B.-J. (2000) Eur. J. Biochem. 267, 2695–2704.
[21] Yoon, M.-K., Park, S.-H., Won, H.-S., Na, D.-S. and Lee, B.-J. (2000) FEBS Lett. 484, 241–245.
[22] Contessi, S., Tanfani, F., Scirè, A., Marelli, I. and Lippe, G. (2001) FEBS Lett. 506, 221–224.
[23] Tanfani, F., Scirè, A., Masullo, M., Raimo, G., Bertoli, E. and Bocchini, V. (2001) Biochemistry 40, 13143–13148.
[24] Makhatadze, G.I., Lopez, M.M., Richardson III, J.M. and Thomas, S.T. (1998) Protein Sci. 7, 689–697.
[25] Ogasahara, K., Lapshina, E.A., Sakai, M., Izu, Y., Tsunasawa, S., Kato, I. and Yutani, K. (1998) Biochemistry 37, 5939–5946.
[26] Burlacu-Miron, S., Perrier, V., Gilles, A.-M., Pistotnik, E. and Craescu, C.T. (1998) J. Biol. Chem. 273, 19102–19107.
[27] Van Asselt, E.J. and Dijkstra, B.W. (1999) FEBS Lett. 458, 429–435.
[28] Masino, L., Martin, S.R. and Bayley, P.M. (2000) Protein Sci. 9, 1519–1529.
[29] Li, Z., Stafford, W.F. and Bouvier, M. (2001) Biochemistry 40, 11193–11201.